Supplemental Text and Figures

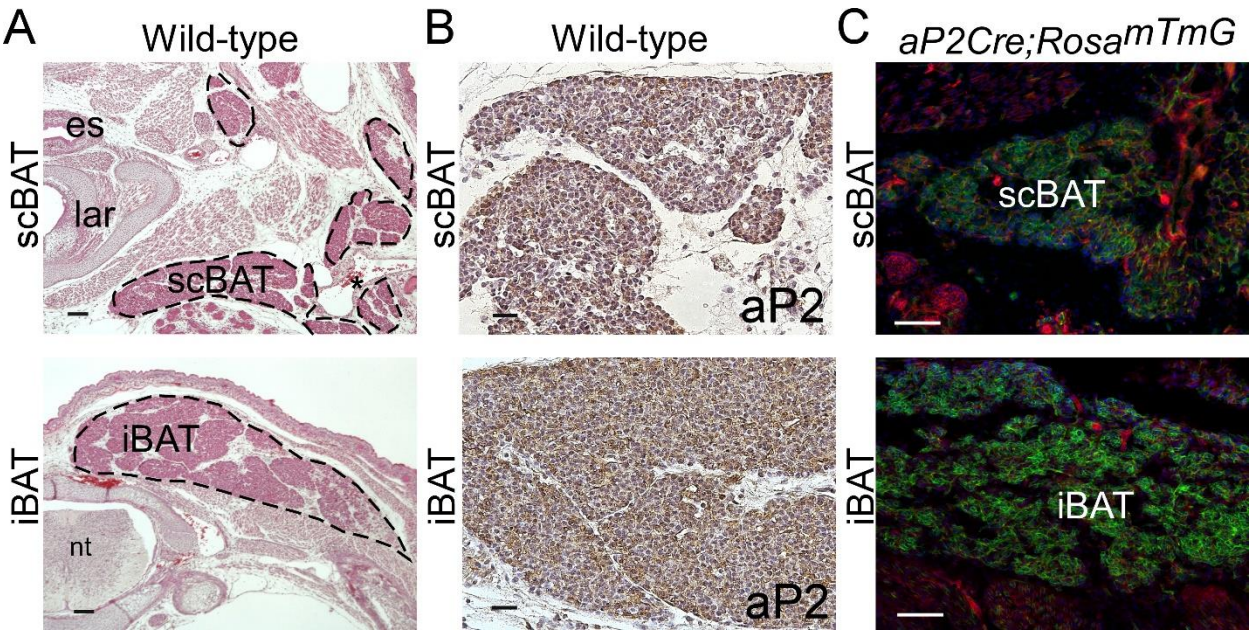

Supplemental Figure 1

scBAT can be readily identified in E16.5 mouse embryos. (A) Representative H&E stained transverse sections from E16.5 mouse embryonic ventral neck and thoracic regions showing anatomical locations of the iBAT and scBAT depots. es: esophagus, lar: larynx, *: external jugular vein, nt: neural tube. n = 4. Scale bar: 200 μm. (B) Immunohistochemistry staining of E16.5 iBAT and scBAT sections using an antibody against aP2/Fabp4. n = 3. Scale bar: 50 μm. (C) Both iBAT and scBAT express Cre in an adipose tissue specific Cre mouse, *aP2/Fabp4-Cre*, at E16.5. Cre recombinase expression is revealed as GFP positive signal (green) in *aP2/Fabp4-Cre; ROSA*^{mTmG} reporter mice. n = 3. Scale bar: 100 μm.

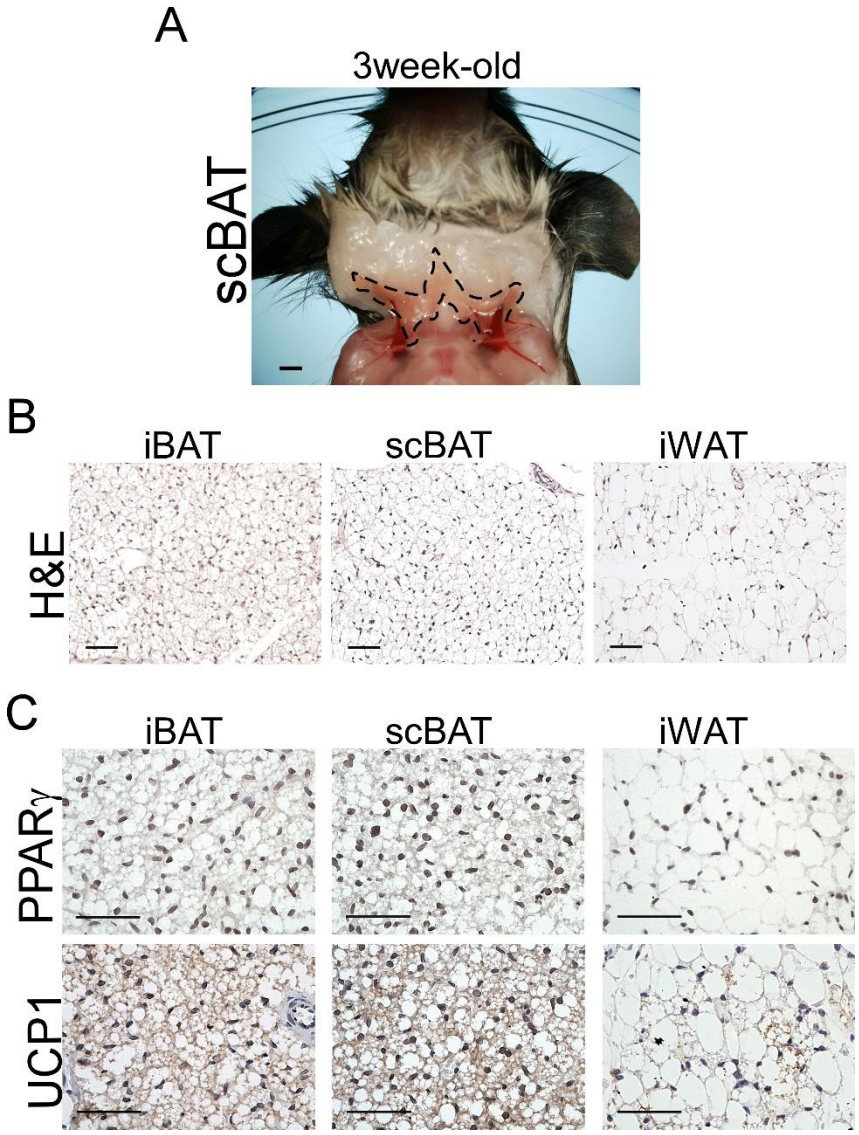

Supplemental Figure 2

Growth of scBAT continues after birth. (A) Representative image showing the anatomical location of scBAT in a 3-week-old mouse (ventral view). scBAT is outlined with the black dotted line. Scale bar: 1000 µm. (B) Representative H&E stained transverse sections of iBAT, scBAT, and iWAT. n = 3. Scale bar: 50 µm. (C) Immunohistochemistry of paraffin embedded iBAT, scBAT, and iWAT sections using antibodies against PPARγ and UCP1. n = 3. Scale bar: 50 µm.

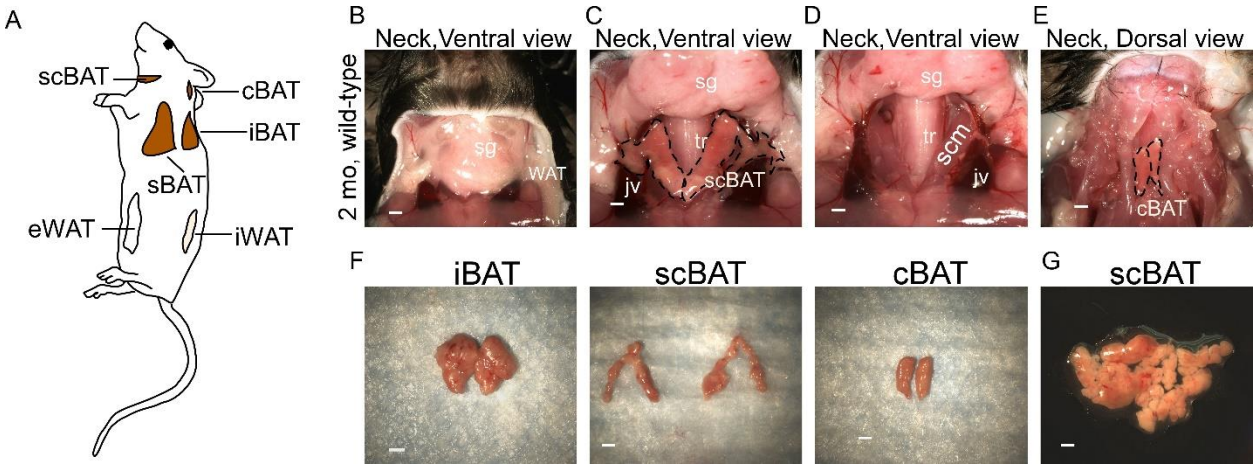

Supplemental Figure 3

Step-by-step illustration of scBAT dissection. (A) Schematic showing the anatomical locations of cBAT, scBAT, iBAT, sBAT, iWAT, and eWAT. (B) The mouse ventral neck after removing skin to reveal the salivary gland, WAT, and superficial muscle. 2 mo: 2 month old (C) scBAT, the jugular vein, and the trachea (covered by sternohyoid muscle) are revealed after the salivary gland is moved upward. (D) Ventral neck image after removing scBAT. (E) cBAT is revealed after removing the skin, WAT, and muscle in the dorsal neck. scBAT and cBAT are outlined with the black dotted line. (F) Images of iBAT, scBAT, and cBAT. (G) Image showing that scBAT is composed of small lobes of brown adipocytes. Scale bar: 1000 μm (B-G).

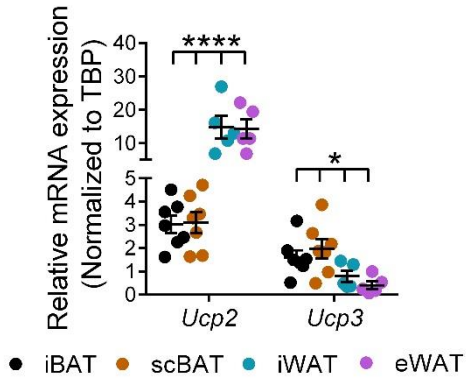

Supplemental Figure 4

Lower expression of *Ucp2 and Ucp3* in scBAT. Relative mRNA expression of *Ucp2* and *Ucp3* in iBAT, scBAT, iWAT, and eWAT isolated from 8-week-old mice. Data are presented as mean ± SEM. n =5-7. ****P< 0.0001, *P< 0.05. One-way ANOVA.

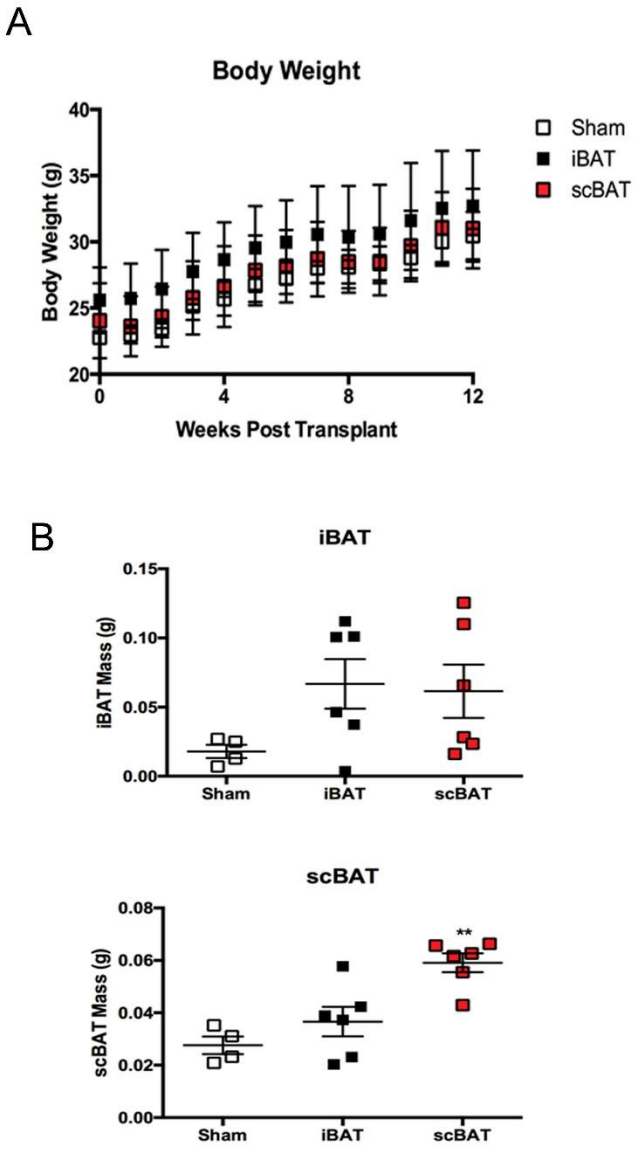

Supplemental Figure 5

Body weight was not reduced in BAT transplanted mice. (A) Body weight (g) and (B) tissue weights of endogenous iBAT and scBAT from BAT transplanted groups and sham-operated group. Data are presented as mean ± SEM. n =4-6. **P < 0.01. One-way ANOVA.

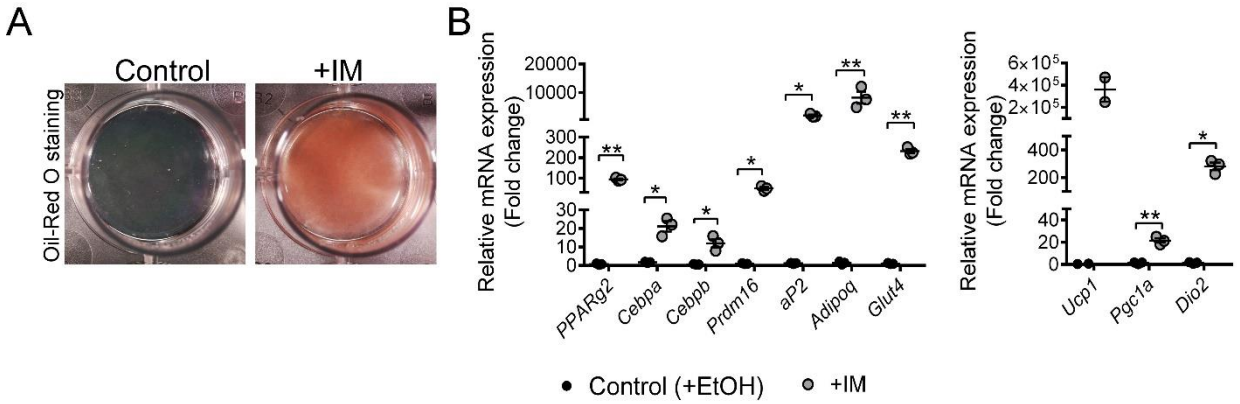

Supplemental Figure 6

Immortalized stromal-vascular fraction (SVF) cells (P7scBAT-C4 cells) isolated from scBAT can differentiate into mature brown adipocytes. (A) Oil-red O staining of lipid droplet accumulation in differentiated P7scBAT-C4 cells. IM: induction medium. (B) Relative mRNA expression of BAT markers in differentiated P7scBAT-C4 cells. Data is presented as mean ± SEM. n =2-3. **P< 0.01, *P<0.05. Two tailed *t* test. Specific gene expression was normalized to b-actin.

Supplemental Table 1: **Biological process gene ontology terms showing statistically significant enrichment in the set of scBAT-specific genes in scBAT v.s. iWAT.**

Term	Count	%	P Value
GO:0006811~ion transport	54	8.035714	1.71E-09
GO:0055114~oxidation reduction	51	7.589286	5.21E-09
GO:0006091~generation of precursor metabolites and energy	46	6.845238	1.46E-21
GO:0006812~cation transport	34	5.059524	5.36E-05
GO:0030001~metal ion transport	30	4.464286	1.00E-04
GO:0055085~transmembrane transport	29	4.315476	4.55E-04
GO:0042592~homeostatic process	28	4.166667	0.022091
GO:0007517~muscle organ development	24	3.571429	4.41E-09
GO:0051186~cofactor metabolic process	24	3.571429	8.47E-09
GO:0015672~monovalent inorganic cation transport	23	3.422619	1.70E-04
GO:0045941~positive regulation of transcription	23	3.422619	0.036426
GO:0015980~energy derivation by oxidation of organic compounds	22	3.27381	1.48E-12
GO:0048878~chemical homeostasis	22	3.27381	0.004465
GO:0005996~monosaccharide metabolic process	21	3.125	1.71E-06
GO:0045893~positive regulation of transcription, DNA-dependent	21	3.125	0.03261
GO:0060537~muscle tissue development	20	2.97619	3.32E-08
GO:0006006~glucose metabolic process	20	2.97619	5.36E-08
GO:0042692~muscle cell differentiation	19	2.827381	1.65E-08
GO:0006631~fatty acid metabolic process	19	2.827381	1.46E-05
GO:0045944~positive regulation of transcription from RNA polymerase II promoter	19	2.827381	0.028435
GO:0022900~electron transport chain	18	2.678571	5.09E-08
GO:0051146~striated muscle cell differentiation	17	2.529762	1.05E-08
GO:0007507~heart development	17	2.529762	0.001457
GO:0050801~ion homeostasis	17	2.529762	0.018821
GO:0007010~cytoskeleton organization	17	2.529762	0.044327
GO:0003012~muscle system process	16	2.380952	1.26E-09
GO:0045333~cellular respiration	15	2.232143	2.00E-09
GO:0006936~muscle contraction	15	2.232143	2.53E-09
GO:0048568~embryonic organ development	15	2.232143	0.016926
GO:0006084~acetyl-CoA metabolic process	14	2.083333	2.22E-12
GO:0006820~anion transport	14	2.083333	1.79E-04
GO:0006813~potassium ion transport	14	2.083333	0.001313
GO:0055001~muscle cell development	13	1.934524	2.66E-07
GO:0055080~cation homeostasis	13	1.934524	0.011355
GO:0015698~inorganic anion transport	12	1.785714	4.41E-05
GO:0006163~purine nucleotide metabolic process	12	1.785714	0.010409

GO:0044057~regulation of system process	12	1.785714	0.046121
GO:0046356~acetyl-CoA catabolic process	11	1.636905	8.89E-10
GO:0048738~cardiac muscle tissue development	11	1.636905	7.90E-06
GO:0016052~carbohydrate catabolic process	11	1.636905	1.79E-04
GO:0048562~embryonic organ morphogenesis	11	1.636905	0.026783
GO:0030036~actin cytoskeleton organization	11	1.636905	0.031006
GO:0006096~glycolysis	10	1.488095	6.05E-06
GO:0007519~skeletal muscle tissue development	10	1.488095	3.40E-04
GO:0051188~cofactor biosynthetic process	10	1.488095	0.00188
GO:0055065~metal ion homeostasis	10	1.488095	0.005276
GO:0016042~lipid catabolic process	10	1.488095	0.022314
GO:0010927~cellular component assembly involved in morphogenesis	9	1.339286	1.05E-05
GO:0006821~chloride transport	9	1.339286	5.21E-04
GO:0009108~coenzyme biosynthetic process	9	1.339286	7.23E-04
GO:0055074~calcium ion homeostasis	9	1.339286	0.008741
GO:0006816~calcium ion transport	9	1.339286	0.03281
GO:0030239~myofibril assembly	8	1.190476	8.93E-07
GO:0006874~cellular calcium ion homeostasis	8	1.190476	0.021715
GO:0035051~cardiac cell differentiation	7	1.041667	4.42E-04
GO:0006112~energy reserve metabolic process	7	1.041667	8.36E-04
GO:0042471~ear morphogenesis	7	1.041667	0.029048
GO:0050873~brown fat cell differentiation	6	0.892857	0.001717
GO:0005977~glycogen metabolic process	6	0.892857	0.003103
GO:0048747~muscle fiber development	6	0.892857	0.005792
GO:0044242~cellular lipid catabolic process	6	0.892857	0.028216
GO:0045444~fat cell differentiation	6	0.892857	0.038876
GO:0055006~cardiac cell development	5	0.744048	6.85E-04
GO:0006090~pyruvate metabolic process	5	0.744048	0.006632
GO:0031214~biomineral formation	5	0.744048	0.021605
GO:0055003~cardiac myofibril assembly	4	0.595238	5.36E-04
GO:0045214~sarcomere organization	4	0.595238	0.00394
GO:0009066~aspartate family amino acid metabolic process	4	0.595238	0.028664
GO:0006941~striated muscle contraction	4	0.595238	0.036022
GO:0034440~lipid oxidation	4	0.595238	0.036022
GO:0014823~response to activity	3	0.446429	0.012985
GO:0006085~acetyl-CoA biosynthetic process	3	0.446429	0.012985
GO:0045426~quinone cofactor biosynthetic process	3	0.446429	0.035919
GO:0007009~plasma membrane organization	3	0.446429	0.035919
GO:0043484~regulation of RNA splicing	3	0.446429	0.035919

Supplemental Table 2. **Sixty-one genes are specifically expressed at higher levels in scBAT v.s. iBAT and WAT (FC > 5, FDR < 0.05).** FC: fold change, FDR: false discovery rate.

EntrezGene	Gene symbol	Gene Name	FC (scBAT/iBAT)	FDR (scBAT/iBAT)
NA	1500016L03Rik	Mus musculus RIKEN cDNA 1500016L03 gene (1500016L03Rik), non-coding RNA.	112.961781	6.41E-08
228151	4833423E24Rik	Mus musculus RIKEN cDNA 4833423E24 gene (4833423E24Rik), mRNA.	51.341769	4.93E-05
233099	Scgb2b27	Mus musculus secretoglobin, family 2B, member 27 (Scgb2b27), mRNA.	39.9200968	1.02E-13
56365	Clcnkb	Mus musculus chloride channel Kb (Clcnkb), mRNA.	39.5130119	0.040356608
12095	Bglap3	NA	39.3878206	4.43E-08
16869	Lhx1	Mus musculus LIM homeobox protein 1 (Lhx1), mRNA.	38.905562	2.43E-27
83380	Prp2	Mus musculus proline rich protein 2 (Prp2), mRNA.	35.0779555	1.60E-05
381819	A630073D07Rik	Mus musculus RIKEN cDNA A630073D07 gene (A630073D07Rik), mRNA.	34.3397601	2.53E-06
11354	Scgb1b27	Mus musculus secretoglobin, family 1B, member 27 (Scgb1b27), mRNA.	33.466295	3.89E-13
22139	Ttr	Mus musculus transthyretin (Ttr), mRNA.	33.4166077	2.09E-07
192200	Wfdc12	Mus musculus WAP four-disulfide core domain 12 (Wfdc12), mRNA.	32.6348831	2.99E-10
16612	Klk1	Mus musculus kallikrein 1 (Klk1), mRNA.	32.0840887	4.75E-06
114600	Gm4736	Mus musculus predicted gene 4736 (Gm4736), mRNA.	30.8516646	4.66E-07
100043232	3110099E03Rik	Mus musculus RIKEN cDNA 3110099E03 gene (3110099E03Rik), non-coding RNA.	30.3842461	5.01E-06
76113	Lpo	Mus musculus lactoperoxidase (Lpo), mRNA.	30.1571661	1.38E-08
12097	Bglap2	Mus musculus bone gamma-carboxyglutamate protein 2 (Bglap2), mRNA.	29.8462468	0.021106693
17844	Mup5	Mus musculus major urinary protein 5 (Mup5), mRNA.	29.76717331	4.84E-11
21419	Tfap2b	Mus musculus transcription factor AP-2 beta (Tfap2b), mRNA.	28.8218361	0.000621104
11571	Crisp1	Mus musculus cysteine-rich secretory protein 1 (Crisp1), mRNA.	28.5843946	1.59E-10
381833	Prb1	Mus musculus proline-rich protein BstNI subfamily 1 (Prb1), mRNA.	28.128162	9.47E-06
192212	Prom2	Mus musculus prominin 2 (Prom2), mRNA.	27.521939	1.84E-06
NA	Chia	Mus musculus chitinase, acidic (Chia), mRNA.	27.2336643	5.48E-11

17830	Prol1	Mus musculus proline rich, lacrimal 1 (Prol1), mRNA.	27.0480639	0.000537072
19131	Prh1	Mus musculus proline rich protein HaeIII subfamily 1 (Prh1), mRNA.	27.0358763	2.83E-05
229722	5330417C22Rik	Mus musculus RIKEN cDNA 5330417C22 gene (5330417C22Rik), mRNA.	26.8335667	2.35653E-05
17341	Bhlha15	Mus musculus basic helix-loop-helix family, member a15 (Bhlha15), mRNA.	25.6052853	4.63E-09
58214	Cst10	Mus musculus cystatin 10 (chondrocytes) (Cst10), mRNA.	25.3060977	3.39E-12
14425	Galnt3	Mus musculus UDP-N-acetyl-alpha-D-galactosamine:polypeptide N-acetylgalactosaminyltransferase 3 (Galnt3), mRNA.	25.2560724	3.66E-05
381832	Prpmp5	Mus musculus proline-rich protein MP5 (Prpmp5), mRNA.	24.8027135	6.06E-07
NA	Gm17495	Mus musculus predicted gene, 17495 (Gm17495), mRNA.	24.1414589	0.000195699
67719	2310057J18Rik	Mus musculus RIKEN cDNA 2310057J18 gene (2310057J18Rik), mRNA.	23.9269215	2.92E-12
18511	Pax9	Mus musculus paired box gene 9 (Pax9), mRNA.	23.0419635	1.42E-06
19752	Rnase1	Mus musculus ribonuclease, RNase A family, 1 (pancreatic) (Rnase1), mRNA.	22.4542834	0.000271902
12353	Car6	Mus musculus carbonic anhydrase 6 (Car6), mRNA.	21.8499984	2.66E-10
13419	Dnase1	Mus musculus deoxyribonuclease I (Dnase1), mRNA.	19.7555411	1.84E-10
110308	Krt5	Mus musculus keratin 5 (Krt5), mRNA.	19.6788821	0.000828969
16538	Kcns1	Mus musculus K+ voltage-gated channel, subfamily S, 1 (Kcns1), mRNA.	19.0723817	0.004888063
232016	Ccdc129	Mus musculus coiled-coil domain containing 129 (Ccdc129), mRNA.	18.8977258	0.006956641
18716	Pip	Mus musculus prolactin induced protein (Pip), mRNA.	18.1745248	1.31E-11
319530	Zfp750	Mus musculus zinc finger protein 750 (Zfp750), mRNA.	17.7800559	0.036627556
330406	B4galnt3	Mus musculus beta-1,4-N-acetyl-galactosaminyl transferase 3 (B4galnt3), mRNA.	17.3181996	0.000461297
140475	Bsnd	Mus musculus Bartter syndrome, infantile, with sensorineural deafness (Barttin) (Bsnd), mRNA.	14.6852147	0.042263563
12023	Barx2	Mus musculus BarH-like homeobox 2 (Barx2), mRNA.	14.6270941	0.0009383
16613	Klk1b11	Mus musculus kallikrein 1-related peptidase b11 (Klk1b11), mRNA.	12.7105542	0.007419035

217294	BC006965	Mus musculus cDNA sequence BC006965 (BC006965), non-coding RNA.	11.6181763	0.004984787
17700	Mstn	Mus musculus myostatin (Mstn), mRNA.	11.3525523	9.78E-05
13711	Elf5	Mus musculus E74-like factor 5 (Elf5), mRNA.	11.1674607	0.000566499
19194	Bpifa2	Mus musculus BPI fold containing family A, member 2 (Bpifa2), mRNA.	9.67263366	6.43E-11
14545	Gdap1	Mus musculus ganglioside-induced differentiation-associated-protein 1 (Gdap1), mRNA.	9.44273111	0.005967238
20599	Smr3a	Mus musculus submaxillary gland androgen regulated protein 3A (Smr3a), mRNA.	8.77579487	7.05E-11
69563	2310015B20Rik	Mus musculus RIKEN cDNA 2310015B20 gene (2310015B20Rik), non-coding RNA.	8.71582535	0.001669507
319894	E330017L17Rik	Mus musculus RIKEN cDNA E330017L17 gene (E330017L17Rik), non-coding RNA.	7.47747957	1.96E-07
NA	1600029D21Rik	Mus musculus RIKEN cDNA 1600029D21 gene (1600029D21Rik), mRNA.	7.33464043	0.002359379
69564	Nmrk2	Mus musculus nicotinamide riboside kinase 2 (Nmrk2), mRNA.	7.15528563	0.010482802
11464	Actc1	Mus musculus actin, alpha, cardiac muscle 1 (Actc1), mRNA.	6.93060129	8.30E-09
20472	Six2	Mus musculus sine oculis-related homeobox 2 (Six2), mRNA.	6.38024811	0.009154531
17879	Myh1	Mus musculus myosin, heavy polypeptide 1, skeletal muscle, adult (Myh1), mRNA.	6.349246781	5.42E-09
68172	Rpl39l	Mus musculus ribosomal protein L39-like (Rpl39l), mRNA.	5.68611274	2.99E-21
382384	Odf3l2	Mus musculus outer dense fiber of sperm tails 3-like 2 (Odf3l2), mRNA.	5.52195678	0.000742083
433294	Mettl21c	NA	5.48069125	0.00826009
545798	Tmem233	Mus musculus transmembrane protein 233 (Tmem233), mRNA.	5.06040033	0.012153065

Supplemental Table 3: **primer sequences used for qRT-PCR**.

Gene symbol	Accession number	Forward Sequences (5'-3')	Reverse Sequences(5'–3')
Actc1	NM_009608	CCAGCCCTCTTTCATTGGTATGGA	TGCCTCCAGATAGGACATTGTTGG
Adipoq	NM_009605	CGTGATGGCAGAGATGGCACTC	AGCGATACACATAAGCGGCTTCTCC
Adrb1	NM_007419	ACGACGACGACGACGACGC	CTTGGACTCCGAGGAGAAGCCC
Adrb2	NM_007420	CTACTGTCGGAGTCCAGATTTCAGGAT	TGCTATTGCTAGAGTAGCCGTTCCC
Adrb3	NM_013462	GCACAGGAATGCCACTCCAATC	TCGAGCATAGACGAAGAGCATCACA
aP2	NM_024406	ACACCGAGATTTCCTTCAAACTG	CCATCTAGGGTTATGATGCTCTTCA
Beta-actin	NM_007393	GGC ACC ACA CCT TCT ACA ATG	GGG GTG TTG AAG GTC TCA AAC
Bglap2	NM_001032298	CAGGAGGGCAATAAGGTAGTGAACAG	CAAGCCATACTGGTCTGATAGCTCGT
Bglap3	NM_001305448	TCCAAGCAGGAGGGCAATAAGGT	CACAAGCAGGGTCAAGCTCACATAG
Bhlha15	NM_010800	GCGCCAGGCCCTAAATTATACCA	GCTGTGGATCTGTGTAGAGTAGCGTTG
Cebpa	NM_007678	AGTACCGGGTACGGCGGGAAC	GCGTGTCCAGTTCACGGCTCA
Cebpb	NM_009883	GGACAAGCTGAGCGACGAGTACAAG	TGCTTGAACAAGTTCCGCAGGG
Cd137	NM_011612	CCAGTACCACCATTTCTGTGACTCCA	ATGAAGATCAGGGCCAGCAGCA
Cd36	NM_001159558	TCCTCTGACATTTGCAGGTCTATCTACG	AGGCATTGGCTGGAAGAACAAATC
Cidea	NM_007702	TCAGACCTTAAGGGACAACACGCA	TGACATTGAGACAGCCGAGGAAGT
Cited1	NM_001276474	CAGGCTCTGAAATGCCAACTATGTC	TTGGAGTAGGCCAGAGAGTTCATCTC
Cox5b	NM_009942	CAGGCACCAAGGAAGACCCTAATCT	CATCGCTGACTCTCGCCTTTGT
Cox8b	NM_007751	AAGCGCCTGCGAAGTTCACAGT	GCTAAGACCCATCCTGCTGGAACC
Cox7a1	NM_009944	AACCGTGTGGCAGAGAAGCAGAA	CAGAGTCAGCGTCATGGTCAGTCTG
Cst10	NM_021405	GTTGTGGCTGGGAAGAACTACTACTTGA	CGTTGATCTGGAAATTACAGATGACCC
Cycs	NM_007808	GGACCAAATCTCCACGGTCTGTTCG	AAATACTCCATCAGGGTATCCTCTCCC
Dio2	NM_010050	TGTGTCTGGAACAGCTTCCTCCTAGA	AAGTCAAGAAGGTGGCATTCGGC
Ebf2	NM_001276387	GCATTTCAGAGTCCACACAAGGAAATAA	ATGCTGTTGCTGGAGGTGCTGTAAT
Glut1	NM_011400	GCAGATGATGCGGGAGAAGAAGG	GCCTTCTCGAAGATGCTCGTTGA
Glut4	NM_009204	CTGATTCTGCTGCCCTTCTGTCCT	GACATTGGACGCTCTCTCTCCAACTT
HoxC8	NM_010466	ACTCGTCTCCCAGCCTCATGTTTC	CTCTAGTTCCAAGGTCTGATACCGGC
HoxC9	NM_008272	GGCAGCAAGCACAAAGAGGAGAA	AGTTCCAGCGTCTGGTACTTGGTGTA
Hsl	NM_001039507	CATGGCTCAACTCCTTCCTGGAAC	TTCAAGGTATCTGTGCCCAGTAAGCC
Kcnk3	NM_010608	CTTCTACTTCGCCATCACCGTCA	TGCCCAGCAGCGCGTAGAACAT
Lhx1	NM_008498	AAGCCCACACGCCATATCCGT	AGCTGTTTCATCCTTCGCTCCTTG
Lhx8	NM_010713	AGACCCTCCAGAAACTGGCAGAAA	TGGTTGGGACTGACGTGTTTCTTATG
Lpl	NM_008509	CCAGGATGCAACATTGGAGAAGC	GCAGGGAGTCAATGAAGAGATGAATG
Klk1	NM_010639	CAGCTCCTGGACTCCTGTTACCATG	CCTCCAACAATTCGAGACTGGACAG
Mstn	NM_010834	GGCCATGATCTTGCTGTAACCTTCC	AGTGCTCATCGCAGTCAAGCCC
Mtus1	NM_001005865	TTCCTTCGGGGCTCAGGAAA	TCGGAGGACAGCACATCTGG
Pax9	NM_011041	GCAGTGAATGGATTGGAGAAGGG	CATGCTGGATGCTGAGACGAAACT
Pgc1a	NM_008904	GTCAACAGCAAAAGCCACAA	TCTGGGGTCAGAGGAAGAGA
Pparg2	NM_011146	AGGGCGATCTTGACAGGAAAGACA	AAATTCGGATGGCCACCTCTTTGC
Prdm16	NM_027504	TCATATGCGAGGTCTGCCACAAGT	TAGTGCTGAACATCTGCCCACAGT
Tbx1	NM_011532	TCGTGAGTGCCTTTGCTCGCT	TGCGTAGCGTCGCCGAGC
Tfap2b	NM_009334	CTGCTAAAGCCGTGTCCGAGTATT	CTGAGCCAGCAGATCCGTAAATTC
TBP	NM_013684	CATTCTCAAACTCTGACCACTGCACC	GAAGCTGCGGTACAATTCCAGAGC

Ucp1	NM_009463	AGCCACCACAGAAAGCTTGTCAAC	ACAGCTTGGTACGCTTGGGTACTG
Ucp2	NM_011671	ATACTCTCCTGAAAGCCAACCTCATG	TCTCGTCTTGACCACATCAACAGG
Ucp3	NM_009464	AAGTTGCTGGAGTCTCACCTGTTTACTG	CATGTATCGGGTCTTTACCACATCC
Zic1	NM_009573	GCGTTCAGAGAACCTCAAGATCCAC	AAAGGTAGGGCTTGTCGCTCGTG
Zfp423	NM_033327	GGCATGGGCGGTACCTTCAAGT	CTTCTGTGGGCACTGCGAGCA

Methods

Animals All mouse experiments (except adipose tissue transplantation experiments) involved using male C57BL/6 mice acquired from the Center for Comparative Medicine Production Colony at Baylor College of Medicine (BCM). For adipose tissue transplantation experiments, 12-week-old male C57BL/6 mice from Charles River Laboratories were used as donor and recipient mice for transplantation by Dr. Stanford's group at Ohio State University (OSU). All animals were maintained on a standard 12-hour light/12-hour dark cycle at 22°C with free access to standard rodent chow and water. Mice were fed a standard mouse diet 5V5R Rodent Diet (LabDiet Inc.) for mice at BCM and 9F 5020 Lab Diet (PharmaServ Inc.) for mice at OSU. All experiments were approved by the Animal Care Research Committees at Baylor College of Medicine and at the Ohio State University. *aP2-Cre* (stock number: 005069) and *ROSA*^{mTmG} (stock number: 007676) mouse lines were acquired from the Jackson Laboratory. Mice were PCR genotyped using the following primers: *aP2-Cre* mouse: forward primer OCH53 5'CTAAGTCCAGTGATCATTGCCAGGGA3', reverse primer OCH54 5'CCGGCAAACGGACAGAAGCA3'. *ROSA*^{mTmG} mouse: forward common primer OCH487 5'CTCTGCTGCCTCCTGGCTTCT3', wild-type reverse primer OCH488 5'CGA GGCGGATCACAAGCAATA 3', and mutant reverse primer OCH489 5'TCAATGGGCGG GGGTCGTT3'.

Embryo processing, histology, and Immunohistochemistry For histological analyses, mouse embryos were collected at various developmental stages, fixed in 4% paraformaldehyde at 4°C overnight, dehydrated in 100% ethanol, and embedded in paraffin. These embryos were sectioned at 6 μm-thickness and stained with Hematoxylin

and Eosin (H&E) or used for immunohistochemistry (IHC) as previously described (1). Primary antibodies used for IHC are rabbit anti-UCP1 (1:50-100 dilution; ab23841, Abcam), rabbit anti-FABP4/aP2 (1:300 dilution; ab13979, Abcam), and mouse anti-PPARγ (1:50-100 dilution; ab59256, Abcam). H&E and IHC stained sections were imaged using a DS-Fi1 camera connected to a Nikon Eclipse 80i stereomicroscope and were processed using Nikon NIS Elements AR 3.2 software.

Isolation of adipose tissues iBAT, iWAT (inguinal WAT), and eWAT (epididymal WAT) were isolated as previously described (2). To isolate scBAT, we first made a skin incision from the sternum to the lower jaw with surgical scissors at the ventral midline. We further opened the skin incision laterally to reveal the ventral neck structures, including subcutaneous WAT, the superficial muscle layer, and the salivary gland. We then removed the superficial muscle layer and moved the salivary gland upward with a pair of forceps to expose the inner neck structures, including the scBAT, jugular veins, sternocleidomastoid muscles, and trachea (covered by the sternohyoid muscle) under the dissecting microscope (SMZ1500, Nikon). scBAT was then carefully dissected free from the connecting veins using a pair of fine forceps. After thoroughly removing any non-adipose tissues from iBAT, scBAT, sWAT, and vWAT, the weights were recorded. For gene expression analyses of scBAT and iBAT from CL316243 treated mice, 12-week old mice received 1 mg/kg daily i.p. injection for 3 days, and adipose tissues were collected 24 hours after the final injection.

Lipid droplet size measurement H&E stained adipose tissue sections from 8-week old mice were imaged at 400x magnification using a DS-Fi1 camera connected to a Nikon Eclipse 80i stereomicroscope. Lipid droplet size in the center area (70 μm x 70 μm) of

each image was measured using the area measurement tool from the Nikon NIS Elements AR 3.2 software. Four to eight adipose tissue sections were randomly selected for the measurement. A total of 1667 lipid droplets from iBAT, 1100 lipid droplets from scBAT, 182 lipid droplets from iWAT, and 28 lipid droplets from eWAT were measured.

RNA isolation and Quantitative RT-PCR (qRT-PCR) Frozen adipose tissues were ground in liquid nitrogen using a pre-chilled mortar and pestle and homogenized in PureZOL RNA isolation reagent (Bio-Rad) using a hand held homogenizer (Pestle Cordless Motor, Kimble Chase). Total RNA was extracted using an Aurum Total RNA Fatty and Fibrous Tissue Kit following the manufacturer's instructions (Bio-Rad). Two µg of total RNA was used to synthesize first-strand cDNA using the SuperScript III First-Strand Synthesis System (Invitrogen). Quantitative PCR reactions were performed using Platinum SYBR Green qPCR SuperMix-UDG (Invitrogen) in a CFX96 Touch Real-Time PCR Detection System (Bio-Rad). The ΔCt method ($2^{-\Delta Ct}$) was used to calculate the relative mRNA expression level of each gene. Specific gene expression was normalized to either b-actin or TATA box binding protein (TBP). Primers used for qRT-PCR are listed in Supplemental table 3.

Protein isolation and western blotting To isolate proteins, frozen adipose tissues were ground in liquid nitrogen and homogenized in RIPA buffer (50 mM Tris pH 7.4, 150 mM NaCl, 5 mM EDTA, 1% Triton X-100, 1% Na Deoxycholate, 0.1% SDS) containing proteinase inhibitor cocktail (Sigma-Aldrich). Protein concentrations were determined using a Pierce BCA protein assay kit (Thermo Fisher Scientific). Western blotting was performed as previously described (3). Briefly, 10-30 ug of protein lysates were subjected to SDS-page gel electrophoresis and transferred to Immune-Blot PDVF membranes (Bio-

Rad). These membranes were further blocked in 5% milk/TBST buffer (50 mM Tris PH 7.5, 150 mM NaCl) overnight at 4°C and incubated with primary antibodies in 3-5% BSA/TBST for 2 hours and with secondary antibodies in 2.5% milk/TBST for 1 hour at room temperature. Membranes were developed using Pierce ECL Plus western blotting substrate (Thermo Fisher Scientific). Primary antibodies used for western blotting are rabbit anti-UCP1 (1:10,000 dilution; ab10983, Abcam), rabbit anti-FABP4/aP2 (1:2000 dilution; 3544, Cell Signaling), mouse anti-PPARγ (1:2000 dilution; sc-7273, Santa Cruz), rabbit anti-COXIV (1:5000 dilution; 4844, Cell Signaling), and rabbit anti-β-actin (1:5000 dilution; 4967, Cell Signaling). Secondary antibodies used in this study include: anti-mouse-HRP (1:5000 dilution, Jackson Immuno Research Laboratory) and anti-rabbit HRP (1:5000 or 1:15,000 (for UCP1) dilution, Jackson Immuno Research Laboratory).

Isolation, immortalization, and differentiation of the stromal vascular fraction (SVF) from supraclavicular BAT Isolation and immortalization of the SVF from scBAT was performed as previously described (3). For immortalization, scBAT from 3 one-week old mice were pooled together. scBAT was dissected out under the dissecting microscope, rinsed briefly with PBS, and minced into small pieces with a blade. Minced tissue was digested in 1 ml of digestion media (0.155 u/mg collagenase D, 0.5 u/g Dispase II, 10 mM CaCl2 in PBS) with shaking at 70 rpm for 30 min at 37°C. After digestion, 10 ml fresh media (DMEM + 10% FBS + Pen/Strep) was added to the tube to neutralize the digestion mixture, which was filtered through a cell strainer (70 μm diameter) to remove any undigested debris and centrifuged at 500 g for 5 min to pellet the stromal-vascular fraction. The top liquid layer containing floating mature adipocytes was aspirated, and the pelleted SVF was wished twice with media and plated onto a 35 mm cell culture plate.

Twenty-four hours after plating, these stromal-vascular cells were washed twice with cold PBS to remove the red blood cells and immortalized with large T antigen following a previously published procedure (3). The immortalized stromal-vascular cells (named P7scBAT-C4 cells) containing supraclavicular brown preadipocytes were cultured in growth media until confluent and differentiated with standard induction medium containing 3-isobutyl-1-methylxanthine (IBMX) (0.5 mM), Dexamethasone (1 µM), Insulin (5 µg/ml), and T3 (1 nM) for 48 hours. Cells were maintained in media containing Insulin and T3 until fully differentiated. Thermogenesis was induced by incubating with 10 µM Isoproterenol for 6 hours. Oil-red O staining was performed as previously described (1).

RNA-sequencing and data analysis Total RNA was isolated from scBAT, iBAT, iWAT, and eWAT using the method described in the section for RNA isolation. After isolation, 500 ng of total RNA from each adipose tissue sample was sent to the Baylor College of Medicine Genomic and RNA profiling Core for quality checks. Two hundred and fifty ng of total RNA was then used to generate double-stranded DNA libraries using the Illumina TruSeq RNA library preparation protocol. Briefly, cDNA was created using the fragmented 3' poly (A) selected portion of total RNA and random primers. Libraries were created from the cDNA by first blunt ending the fragments, attaching an adenosine to the 3' end, and ligating unique adapters to the ends. The ligated products were then amplified using 15 cycles of PCR. The resulting libraries were quantitated using a NanoDrop spectrophotometer, and fragment size was assessed with an Agilent 2100 Bioanalyzer. A qPCR assay was performed on the libraries to determine the concentration of adapter ligated fragments using the Applied Biosystems ViiA 7 Quantitative PCR instrument and a KAPA Library Quant Kit. All samples were pooled at equimolar amounts, re-quantified

by qPCR, and re-assessed on the Bioanalyzer. Using the pooled concentration from the qPCR assay, the library pool was loaded onto two rapid run flow cells, each at a concentration of 11pM for on-board cluster generation and paired-end sequencing on a HiSeq 2500 at a read length of 100 bp. For mapping and analyzing gene expression, 11 low-quality nucleotides from the 5' ends of the raw reads were trimmed. The resulting 90-nucleotide paired-end reads were mapped to the mouse genome (mm10) using STAR (4) with NCBI RefSeq genes as the reference. In order to reduce possible PCR biases, read duplicates were removed using picard tools (http://broadinstitute.github.io/picard/). HTseq (http://www-huber.embl.de/users/anders/HTSeq) was used to determine the number of reads mapping to known genes. EdgeR (5) was used to analyze the gene-based read counts to detect differentially expressed genes between different adipose tissue samples. The false discovery rate (FDR) of the differentially expressed genes was estimated using Benjamini and Hochberg method. FDR < 0.05 was considered statistically significant. The heat map and principal component analysis (PCA) for Figure 6C and 6D were conducted using R. Venn diagrams were constructed using VENNY[2.1] (http://bioinfogp.cnb.csic.es/tools/venny/index.html) and Gene ontology enrichment was determined using DAVID 6.7 to analyze biological process enrichment in the set of genes with 5 fold higher expression in scBAT than in iWAT (FDR < 0.05) (6, 7). The heat map for Figure 7A was conducted with Multi-experiment Viewer 4.9.0 (MeV).

Transmission electron microscopy (TEM) Adipose tissues were immediately fixed in modified Karnovsky's fixative (2% paraformaldehyde plus 2.5% glutaraldehyde in 0.1M cacodylate buffer) after isolation, and minced into blocks. WAT was fixed under vacuum for 3 hours; BAT was fixed at normal pressure for 3 hours. Both tissues were then left

overnight in weak fixative (1:10) at 4°C. The next day, tissue blocks were rinsed in 0.1M cacodylate buffer and osmicated for 1 hour. Blocks were then rinsed in dH2O and dehydrated through a gradient series of ethanols until 100% ethanol was reached. Blocks were then embedded in Spurr's Low Viscosity resin (8) and polymerized at 60 °C for 3 days. Thin sections were cut using a Diatome Ultra45 knife on a RMC MT6000-XL ultra-microtome, and 60nm sections were collected on 150 hex mesh copper grids. Grids were stained in saturated aqueous uranyl acetate and counter-stained in Reynold's lead citrate (9). Grids were examined on a JEOL 1230 transmission electron microscope, and images were captured using a Gatan US1000 digital camera and Digital Micrograph v1.82.366 software.

BAT transplantation Transplantation was performed using BAT removed from the interscapular (iBAT) or supraclavicular (scBAT) region of 12-week-old male C57BL/6 mice. After euthanasia of donor mice by cervical dislocation, BAT was removed and incubated in 10 ml saline at 37°C for 20–30 minutes. Twelve-week-old C57BL/6 recipient mice were anesthetized with isoflurane. For each recipient mouse, 0.1g of donor BAT (iBAT or scBAT) was transplanted into the visceral cavity. The transplant was carefully lodged deep between folds within the endogenous epididymal fat of the recipient (10, 11). Mice that were sham operated underwent the same procedure, but instead of receiving BAT, their epididymal fat pad was located, exposed, and then replaced.

Glucose (GTT) and Insulin (ITT) Tolerance Tests For glucose tolerance tests, mice were fasted for 11 hours (22:00–9:00) with free access to drinking water. A baseline blood sample was collected from the tail of fully conscious mice, followed by i.p. injection of glucose (2.0 g/kg body weight). Blood was taken from the tail at 15, 30, 60, 90, and 120

minutes after injection. ITTs were performed at 12 weeks after transplantation. Mice were fasted for 2 hours (12:00–14:00), and baseline blood samples were collected from the tail of fully conscious mice. Insulin (1 U/kg body weight) (Humulin; Eli Lilly) was administered by i.p. injection, and blood samples were taken from the tail at 10, 15, 30, 45, and 60 minutes after injection. Glucose concentrations were determined from blood using a OneTouch Ultra portable glucometer (LifeScan).

Core body temperature measurement For BAT transplanted mice, mice were fasted overnight, and body temperature was determined using an animal rectal probe connected to a TH-8 thermometer (Physitemp). Basal temperature was determined, and animals were then placed at 4°C, and body temperature was measured at 15, 30, 60, 90, and 120 minutes.

Statistical analyses The two tailed *t* test was used to evaluate statistical significance between 2 groups. One-way ANOVA was used to evaluate statistical significance between 3 or more groups. A P value less than 0.05 was considered statistically significant. Statistical analyses were performed using GraphPad Prism 6 software.

Study Approval All animal experiments were approved by the Institutional Animal Care and Use Committees of Baylor College of Medicine (BCM) and the Ohio State University.

References

1. Nosavanh L, Yu DH, Jaehnig EJ, Tong Q, Shen L, and Chen MH. Cell-autonomous activation of Hedgehog signaling inhibits brown adipose tissue development. *Proc Natl Acad Sci U S A.* 2015;112(16):5069-74.

2. de Jong JM, Larsson O, Cannon B, and Nedergaard J. A stringent validation of mouse adipose tissue identity markers. *Am J Physiol Endocrinol Metab.* 2015;308(12):E1085-105.

3. Chen MH, Wilson CW, Li YJ, Law KK, Lu CS, Gacayan R, et al. Cilium-independent regulation of Gli protein function by Sufu in Hedgehog signaling is evolutionarily conserved. *Genes Dev.* 2009;23(16):1910-28.

4. Dobin A, Davis CA, Schlesinger F, Drenkow J, Zaleski C, Jha S, et al. STAR: ultrafast universal RNA-seq aligner. *Bioinformatics.* 2013;29(1):15-21.

5. Robinson MD, McCarthy DJ, and Smyth GK. edgeR: a Bioconductor package for differential expression analysis of digital gene expression data. *Bioinformatics.* 2010;26(1):139-40.

6. Huang da W, Sherman BT, and Lempicki RA. Systematic and integrative analysis of large gene lists using DAVID bioinformatics resources. *Nat Protoc.* 2009;4(1):44-57.

7. Huang da W, Sherman BT, and Lempicki RA. Bioinformatics enrichment tools: paths toward the comprehensive functional analysis of large gene lists. *Nucleic Acids Res.* 2009;37(1):1-13.

8. Spurr AR. A low-viscosity epoxy resin embedding medium for electron microscopy. *J Ultrastruct Res.* 1969;26(1):31-43.

9. Reynolds ES, Tomkiewicz ZM, and Dammin GJ. The Renal Lesion Related to Amphotericin B Treatment for Coccidioidomycosis. *Med Clin North Am.* 1963;47:1149-54.

10. Stanford KI, Middelbeek RJ, Townsend KL, An D, Nygaard EB, Hitchcox KM, et al. Brown adipose tissue regulates glucose homeostasis and insulin sensitivity. *J Clin Invest.* 2013;123(1):215-23.

11. Tran TT, Yamamoto Y, Gesta S, and Kahn CR. Beneficial effects of subcutaneous fat transplantation on metabolism. *Cell Metab.* 2008;7(5):410-20.